RESEARCH PAPER

Design, Optimization Process and Efficient Analysis for Preparation of Copolymer-Coated Superparamagnetic Nanoparticles

Mahnaz Mahdavi shahri [1], * and Susan Azizi [2]

[1] *Department of Chemistry, Shiraz Branch, Islamic Azad University, Shiraz, Iran*

[2] *Department of Bioprocess Technology, Faculty of Biotechnology and Biomolecular Sciences, University Putra Malaysia, UPM Serdang, Selangor 43400, Malaysia*

ARTICLE INFO

ABSTRACT

Magnetic nanoparticles (MNPs) are very important systems with potential use in drug delivery systems, ferrofluids, and effluent treatment. In many situations, such as in biomedical applications, it is necessary to cover inorganic magnetic particles with an organic material, such as polymers. A superparamagnetic nanocomposite Fe_3O_4/poly(maleic anhydride-co-acrylic acid) P(MAH-co-AA) with a core/shell structure was successfully synthesized by a dispersion polymerization route. Iron oxide nanoparticles were used as a core, and P(MAH-co-AA) as a shell was covered on the surface of the Fe_3O_4 magnetic nanoparticles. Scanning electron microscopy (SEM) and transmission electron microscopy (TEM) showed that the Fe_3O_4/P(MAH-co-AA) magnetic nanocomposite were highly uniform in size and cubic shape with the average size about 17.06 nm. X-ray diffraction confirmed magnetite cores and also indicated that the binding process did not change the phase of Fe_3O_4. Vibrational sample magnetometer (VSM) revealed the nanoparticles were superparamagnetic and the saturation magnetization was 83.6 and 46.6 emu g^{-1} for pure Fe_3O_4 and composite nanoparticles, respectively. Measurements by VSM also showed that the degree of saturation magnetization increased with increasing iron oxide concentration from 1% to 7 wt % of Fe_3O_4.

How to cite this article

INTRODUCTION

Nanomaterials have received much recent attention because they are expected to be used in various applications based on their excellent and unique optical, electrical, magnetic, catalytic, biological, or mechanical properties [1]. Such properties originate from the finely tuned nanoarchitectures and nanostructures of these materials. Application of nanomaterials could help improve the environment and control pollution, which further progresses environmental science and engineering [2].

Polymer nanocomposites are potentially important due to the fact that they offer a number of significant advantages over traditional polymer composites. Magnetic polymer nanocomposites are usually composed of magnetic cores to ensure a strong magnetic response and polymeric shells to provide favorable functional groups and protect the magnetic nanoparticles against environmental degradation effects and isolate these blocks from each other to weaken and/or avoid the

* *Corresponding Author Email: mahnaz.chem@gmail.com*

magnetic interaction [3]. The use of nanoparticles in polymeric systems has become a subject of interest in engineering applications due to potential dramatic changes in physical properties of composites. These changes in properties come from two aspects of nanoparticles: increased surface area and quantum effects associated with nano-dimensional particle structures [4]. These factors can change or enhance properties such as reactivity, strength, and electromagnetic properties of composites. The presence of nanoparticles also provides improvements in other properties as well, such as erosion resistance, wear resistance, fire resistance, hardness, and environmental resistance.

The application in biomedicine and bioengineering fields is also new progress due to they can be easily collected with the application of a magnetic field; and the coupling of appropriate ligands to such microspheres provides an effective tool to achieve rapid, simple, and specific biological separation [5].

Currently, magnetically controlled drug targeting has become one of the most active areas of cancer research since it offers true possibilities of active drug targeting and selective guidance of anticancer drug molecules to specific cells of the diseased site. The basic challenge in drug delivery is the transfer of drug agents to targeted sites at an appropriate time [6]. Apart from the application in drug controlled release, the magnetic polymer composites have also found wide applications in adsorbents of heavy metal ions and organic pollutants in waste water so that the strong magnetism is in favor of the separation and recycle of adsorbents [7]. Because of comparatively large surface areas, it is likely that nanosized adsorbents with strong affinity can be a useful tool in enhancing the adsorption capacity in drinking water treatment [8]. Applications of nanomaterials in environmental protection have created conditions to improve environment and control pollution, which will bring breakthrough progress to environmental science and engineering.

In this work, poly(maleic anhydride-co-acrylic acid) P(MAH-co-AA) was chosen as a polymer shell onto the magnetite nanoparticle because it offers the possibility to anchor additional functional groups for active site attachment. The morphology, magnetic properties and optimized condition of the magnetic nancomposite were examined with a FTIR, SEM, TEM, XRD and VSM.

MATERIALS AND METHODS
Materials

All the chemicals were analytical purity and used without further purification. Iron (III) chloride hexahydrate ($FeCl_3.6H_2O$), iron (II) sulfate heptahydrate ($FeSO_4.7H_2O$), the ammonium hydroxide (NH_4OH) solution (25 wt%) and oleic acid (OA) were purchased from the Bendosen Laboratory Chemicals,Malaysia. The monomers maleic anhydride (MAH) and acrylic acid (AA) were obtained from Fluka, Sigma-Aldrich, Switzerland. 2,2-azo-bisisobutyronitrile (AIBN), polyvinylpyrrolidone (PVP), 1,4-dioxane and N,N-methylenebisacrylamide (BIS) were purchased from Sigma-Aldrich, U.S.A. All chemicals are analytical grade without further purification. Deionized water was used throughout the experiments.

Synthesis of Modified Magnetite Nanoparticles

The Fe_3O_4 magnetite nanoparticles (Fe_3O_4-MNPs) were prepared by a co-precipitation method [9]. A bout 0.046 mol of $FeCl_3$-$6H_2O$ and 0.023 mol of $FeSO_4$-$7H_2O$ were dissolved into 150 mL deionized water in 250 mL three-necked flask and nitrogen gas was bubbled for 3 min to extrude the air. Then 20 mL ammonium hydroxide was added quickly into the iron solution under vigorous stirring. After 30 min 3 mL oleic acid was added into the mixture to modify the Fe_3O_4 MNPs and the mixture was heated to 80°C. After 1h, the resulting Fe_3O_4 nanoparticles (black precipitate) were collected from the solution by magnetic separation and washed several times with deionized water and ethanol, then dried under vacuum conditions at 60 °C for 12h. The pH range of the synthesis iron oxide NPs should be 8-14 with maintaining molar ratio of Fe^{3+}/Fe^{2+} (2:1) under a non-oxidizing condition. It is important to have an oxygen free environment during the synthesis otherwise; magnetite can be further oxidized to ferric hydroxide in the reaction medium. In the absence of any surface modification Fe_3O_4-MNPs tend to aggregate due to strong magnetic dipole-dipole attractions between particles.

Synthesis of Magnetic Fe_3O_4/P(MAH-Co-AA) Core/ Shell Nanocomposites

The magnetic Fe_3O_4/P(MAH-co-AA) core/shell nanocomposites were prepared using a dispersion polymerization method. First, in a 150 mL three-neck flask, different concentration of modified Fe_3O_4 nanoparticles were dispersed in 10 mL 1,4-dioxane solution and the solution mixture was ultrasonicated

for 20 min, and then mechanically stirred at 45 °C under nitrogen. In another flask, 0.4 g MAH, 0.4 mL AA, and 0.15 g PVP as stabilizer were dispersed in 20 mL 1,4-dioxane under ultrasonication for 30 min. Subsequently, the mixture was rapidly added into the previous ferrofluid and the stirring speed was adjusted to 500 rpm. Then 0.02 g AIBN as an initiator and 0.05 g BIS as a cross-linker were added into the reaction mixture. The resulting medium was transferred into the reactor and sonicated for about 5 min within an ultrasonic water bath for the complete dissolution of AIBN in the polymerization medium.

The polymerization reactor was placed in a water bath and heated to 75°C for 6 h with a mechanical stirring (500 rpm). The whole process was protected in nitrogen. After the reaction, a brown-colored product was separated from the solution by magnetic separation. The particles were sequentially washed with acetone and deionized water several times and vacuum-dried at 60 °C for 24h to obtain the polymer-coated Fe_3O_4 magnetic nanocomposite.

*Characterization Methods and Instruments*

Fourier transform infrared spectroscopy (FTIR) was used to identify the functional groups present in the synthesized compounds. FTIR spectra were recorded over the range of (400-4000) cm^{-1} with a Perkin Elmer 1650, FTIR spectrophotometer. The crystal structure of the samples prepared has been confirmed by XRD analysis with a Shimadzu XRD-6000 Lab X wideangle diffractometer. The average particle size and size distribution of the samples were observed by a Hitachi H-7100 transmission electron microscope (TEM) with an acceleration voltage of 200 kV, whereas the particle size distributions were determined using the UTHSCSA Image Tool version 3.00 program. The analysis of the surface morphologies of the samples was performed with a Philips XL-30 environmental scanning electron microscope (SEM). Magnetization measurements were carried out with a Lakeshore (model 7407) vibrating sample magnetometer (VSM) to study magnetic properties of the magnetic nanoparticles under magnetic fields up to 10KG (1T) at room temperature.
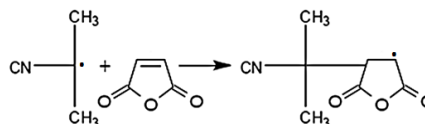
RESULTS AND DISCUSSION

In this work, AIBN used as the initiator in the dispersion polymerization to synthesize Fe_3O_4/poly(maleic anhydride-co-acrylic acid) magnetic

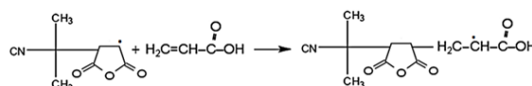nanocomposite with core/shell structure. The mechanism for polymerization is shown below:
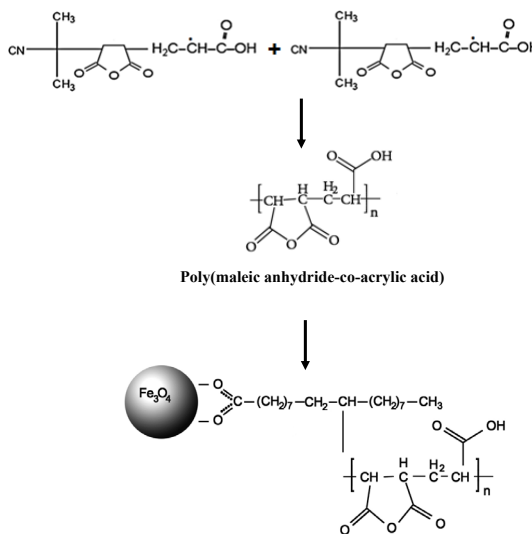
1) Free radical formation from initiator
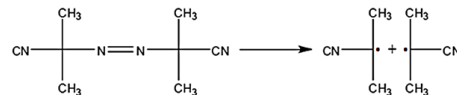
2) Addition of free radical to monomer

3) Propagation of polymer chain

4) Termination of chain via coupling

Poly(maleic anhydride-co-acrylic acid)

The schematic structures for the formation of magnetic Fe_3O_4/P(MAH-co-AA) core/shell nanocomposites is shown in Fig. 1. The first step is the formation of Fe_3O_4 nanoparticles by precipitation and coating with oleic acid as stabilizing agent. The second step is encapsulation of magnetic nanoparticles into P(MAH-co-AA) by dispersion polymerization to form a magnetic core with a polymer shell.

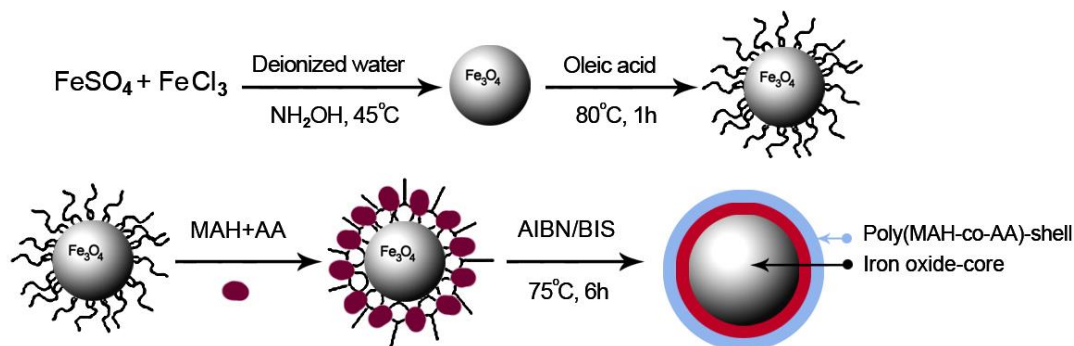*Structural Analysis of Magnetic Fe_3O_4/P(MAH-Co-AA) Core/Shell Nancomposites*

Fig. 1. Schematic illustration for the preparation of magnetic Fe₃O₄/P(MAH-co-AA) core/shell nanocomposites.

Fourier Transform Infrared Spectroscopy

FTIR spectra of the Fe_3O_4 nanoparticles, and magnetic Fe_3O_4/P(MAH-co-AA) core/shell are shown in Fig. 2. For the IR spectrum of Fe_3O_4 nanoparticles (Fig. 2a), the strong IR band of magnetite is Fe-O stretching at 580 cm^{-1} and the absorption peak around 3440 cm-1 is attributed to the hydroxyl groups on the surface of Fe_3O_4 or adsorbed water [10-11]. The presence of additional peaks is related to OA-coated magnetite nanoparticles [9]. The characteristic bands of the anhydride cycles are observed at 1860, 1784 cm^{-1} due to the C=O bonded with non-conjugated oxygen atoms [12]. The absorption bands of the carboxyl groups of PAA can be noticed at 2960 cm^{-1} and 1675 cm^{-1} correspond to O-H and C=O stretching vibration respectively in the IR spectrum of the P(MAH-co-AA). In addition, AA and MAH show two peaks at 1169 and 1285 cm^{-1} due to the C-O stretching. The results indicate that P(MAH-co-AA) was successfully synthesized. The absorption bands at 580 cm-1 of the Fe–O bond (Fig. 2b), combined with the characteristic peaks at 2960, 1784 and 1675 cm^{-1}, signify that P(MAH-co-

AA) was successfully polymerized and the active groups has been introduced onto the surface of magnetite core. Therefore the magnetite Fe_3O_4 surface was wrapped by the copolymer P(MAH-co-AA) and a novel magnetic Fe_3O_4/P(MAH-co-AA) nanocomposite has been synthesized.

X-ray Diffraction

Fig. 3 shows the XRD patterns for Fe_3O_4 nanoparticles and P(MAH-co-AA). A series of characteristic peaks for Fe_3O_4 nanoparticles were observed in the XRD pattern at 2θ of 9.6°, 30.1°, 35.9°, 43.8°, 54.5°, 57.6° and 63.6°. The positions and relative intensities of the reflection peak of Fe_3O_4 nanoparticles agree with the XRD diffraction peaks of standard Fe_3O_4 samples indicating that the black-colored magnetic powders are Fe_3O_4-MNPs [13]. Sharp peaks in Figure 3a suggest that the Fe_3O_4-MNPs have good crystallize structure. It was found that the magnetite crystallites could be well indexed to the inverse cubic spinel structure of Fe_3O_4. The broader peak at 2θ of 20.5o could be assigned to the diffraction scattering of amorphous P(MAH-co-AA) copolymers (Fig. 3b).

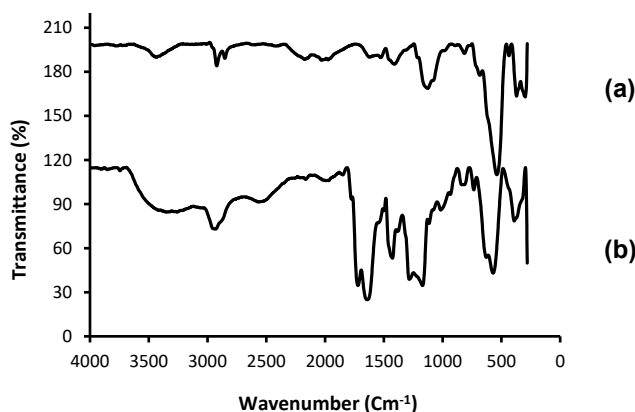Fig. 2. FT-IR spectra of (a) Fe₃O₄-MNPs, and (b) magnetic Fe₃O₄/P(MAH-co-AA) core/shell nanocomposite

The peak intensity of Fe_3O_4/P(MAH-co-AA) nanocomposite is lower than that of pure Fe_3O_4 nanoparticles in order to the Fe_3O_4 nanoparticles are incorporated into polymer spheres. It is clear from Fig. 4, the peak intensity of polymer increases by decreasing concentration of Fe_3O_4-MNPs and polymer peak is clearer from a-d. It can be explained that polymer thickness increases by decreasing of nanoparticle concentration, therefore peak intensity of polymer better detected. On the other hand reduction peak intensity of polymer is due to polydispertion in high concentration of Fe_3O_4.

The average crystal sizes of the Fe_3O_4 and Fe_3O_4/P(MAH-co-AA) core/shell nanocomposite were calculated from the XRD data using Debye-Scherrer equation, and found to be 9.2 and 15.15 nm, respectively.

Transmission Electron Microscopy

TEM image of the magnetite nanoparticles shows that the sizes of Fe_3O_4 nanoparticles are almost uniform and most of the particles are approximately cubic in shape. As shown in Fig. 5a, the particle size distribution curve of Fe_3O_4 MNPs indicated that mean diameter size was 9.41 nm.

Fig. 5b shows TEM images of polymer coated magnetite nanoparticles. It is clear from the TEM images that Fe_3O_4/P(MAH-co-AA) nanoparticles used in this case have excellent dispersibility and the composite particles are cubic in shape and the magnetic particles are encapsulated in the P(MAH-co-AA) template. No pure polymer particles are observed. It can be seen from Fig. 5a; the pure Fe_3O_4 MNPs were polydisperse and seriously aggregated. After surface polymerization the dispersion of Fe_3O_4 nanoparticles improved greatly, which can be explained by the fact that the interaction among particles might be changed after modification with P(MAH-co-AA), leading to good dispersion. Histogram evaluating size distributions of the polymer coated nanoparticles
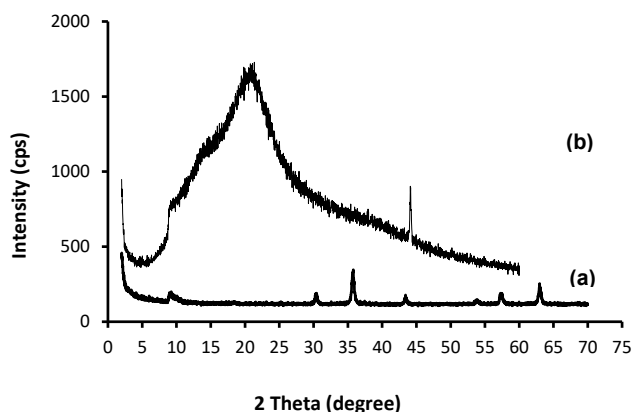

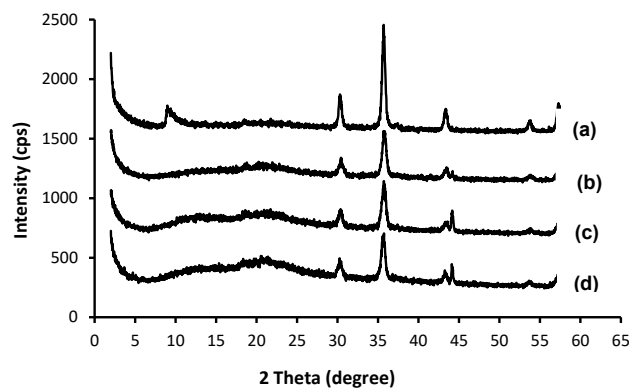Fig. 3 XRD patterns of pristine (a) Fe_3O_4-MNPs, and (b) P(MAH-co-AA)

Fig. 4 XRD patterns of magnetic Fe_3O_4/P(MAH-co-AA) core/shell nanocomposite at different concentration of Fe_3O_4-MNPs with (a) 1.0, (b) 3.0, (c) 5.0, and (d) 7.0 wt% of P(MAH-co-AA).

showed that the average particle size was 17.09 nm, and the results were reasonably consistent with those obtained from XRD. It should be noted that the average size of core/shell nanoparticles was higher than that of naked Fe_3O_4 nanoparticles; therefore it is clear that the average particle size increased after surface modification.

Transmission Electron Microscopy of Nanocomposites at Different Concentration of Fe_3O_4-MNPs

Magnetic polymer nanocomposite with different magnetic content were synthesised by reacting different amounts of Fe_3O_4 nanoparticles. Increasing the concentration of magnetic nanoparticles, results in an increase of polydispersity and the average diameter size from 6.56 to 25.21 nm as shown in Fig. 6. Possibly, the content of the Fe_3O_4-MNPs in the nanocomposites have a considerable effect on the morphology of product due to the existence of static magnetic attraction [14]. Another reason for increasing the magnetic aggregation or magnetic size by increasing magnetite concentration could be that

with rising iron oxide concentration agglomeration is favored compared to encapsulation inside the polymer. As result only few large aggregates are faced to many monomer droplets which cannot encapsulate the iron oxide particles. This decreases monodispersity and increases polydispersity.

Scanning Electron Microscopy

The morphology and structure of the Fe_3O_4 nanoparticles and Fe_3O_4/P(MAH-co-AA) nanocomposite were observed by SEM images as shown in Fig. 7. The results demonstrate that Fe_3O_4 nanoparticles are cubic and highly uniform in size. The SEM micrograph of magnetice Fe_3O_4/P(MAH-co-AA) presented in Fig. 7b shows that the nanocomposite have a porous surface structure. The magnetic nano composites are spherical in shape and have a rough surface due to the pores, which formed during the polymerization process. The porous surface structure is a factor for increasing surface area.
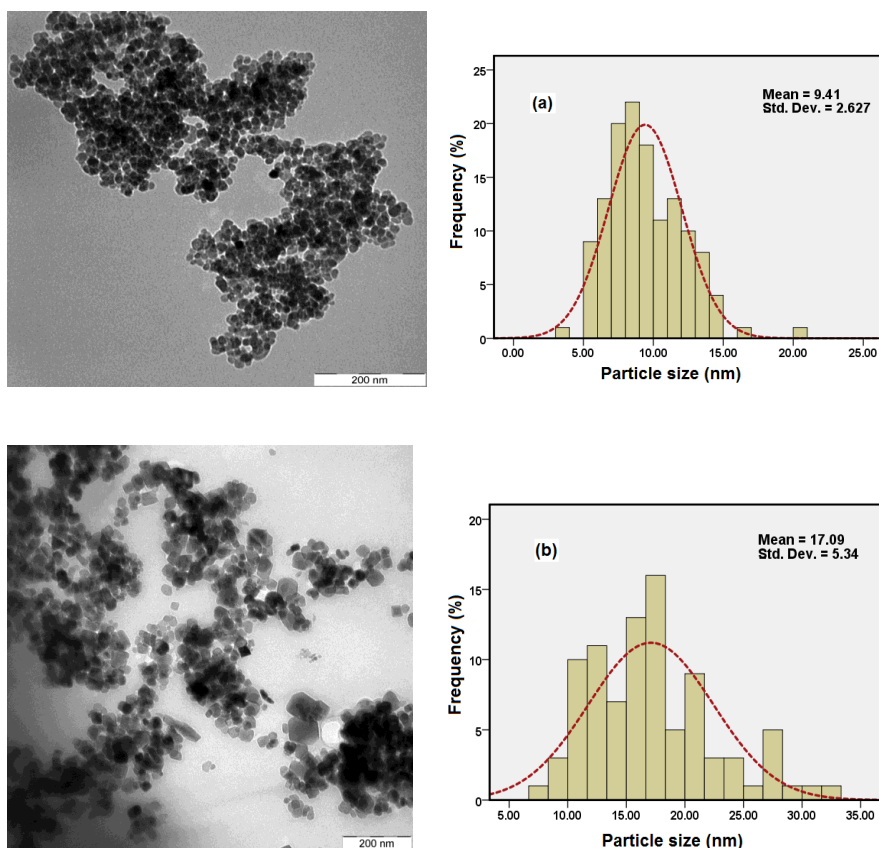

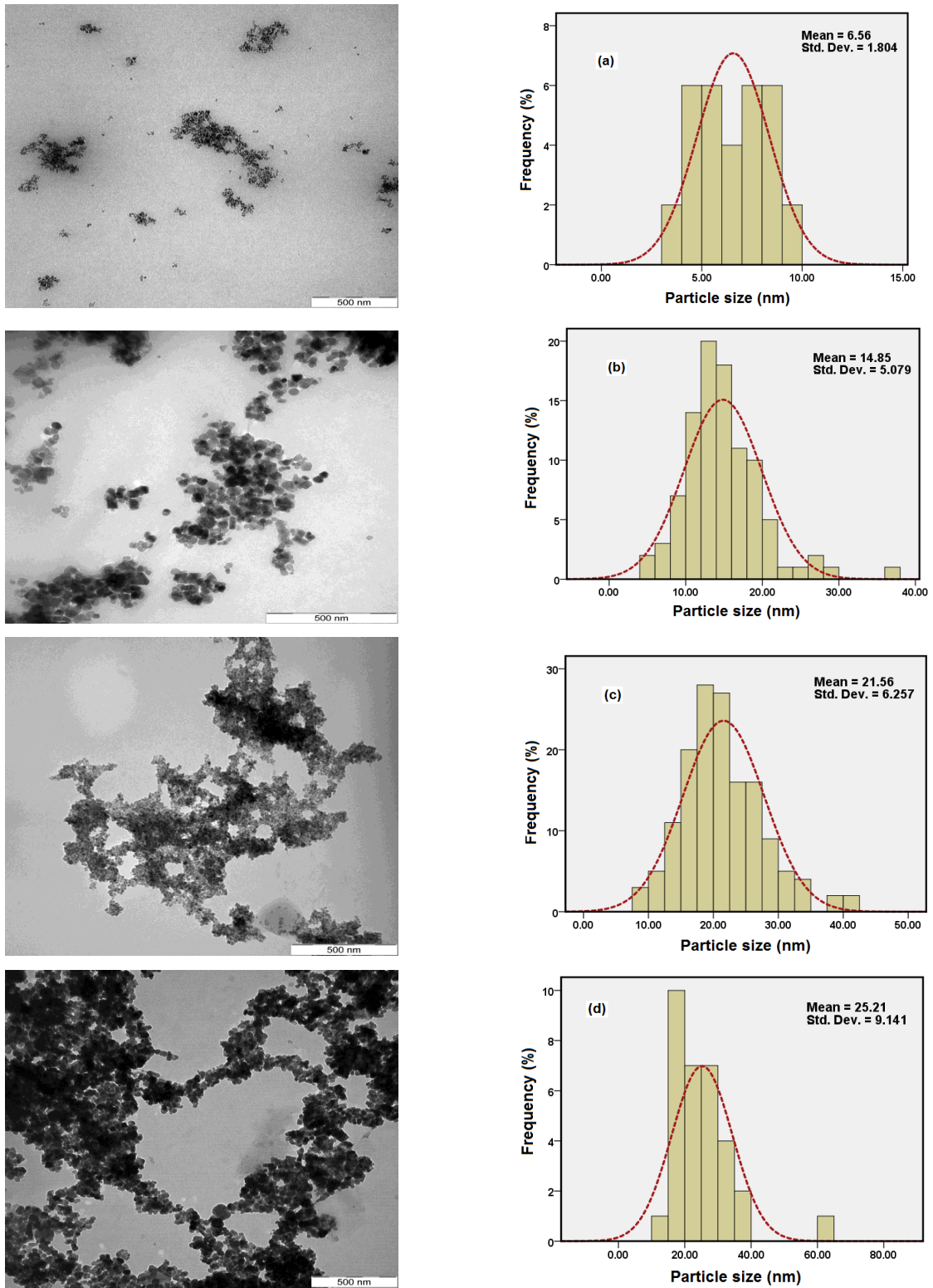Fig. 5 TEM images and their corresponding size distributions of (a) pristine Fe_3O_4, and (b) magnetic Fe_3O_4/P(MAH-co-AA) core/shell nanocomposite.

Fig. 6 TEM images and their corresponding size distributions of Fe$_3$O$_4$/P(MAH-co-AA) at different concentration of Fe$_3$O$_4$-MNPs with (a) 1.0, (b) 3.0, (c) 5.0, and (d) 7.0 wt% of P(MAH-co-AA).

Vibrating Sample Magnetometer

The magnetization curves measured at room temperature for Fe_3O_4 nanoparticles and polymer-coated Fe_3O_4 are compared in Fig. 8. There was no hysteresis in the magnetization for both of samples, suggesting the magnetic particles produced are superparamagnetic and the single-domain magnetite nanoparticles remained in the polymer particles. This can be attributed to the small size of MNPs which were smaller than the superparamagnetic critical size (25 nm). On the other hand when the magnetic component size of the particles is smaller than critical size, the particles will exhibit superparamagnetism [15]. From the magnetization curves, we can also conclude that magnetite nanoparticles were trapped in the polymer matrix without obvious aggregation, which were match with the results of TEM micrographs. The high saturation magnetization of pure Fe_3O_4 indicated the good crystal structure. The saturation magnetization values (M_s) of polymer-coated Fe_3O_4 was smaller than the value for the pure magnetite nanoparticles and decreases from 83.6 to 46.6 emu g^{-1}, therefore the saturation magnetization reduced after polymer coating onto the surface of Fe_3O_4 core. This was due to the existence of the large amount of diamagnetic of the polymer shells surrounding the magnetite nanoparticles [16]. With such high magnetization and superparamagnetic behaviors, the magnetic polymer particles could be easily and rapidly separated from the solution and easily
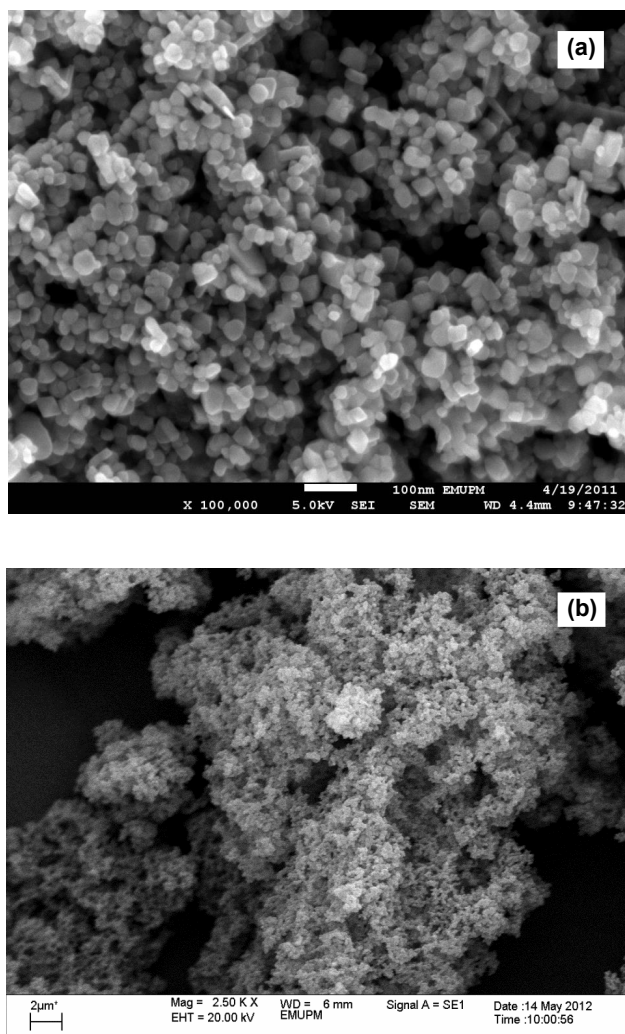

Fig. 7 SEM micrograph of (a) Fe_3O_4-MNPs, and (b) magnetic Fe_3O_4/P(MAH-co-AA) core/shell nanocomposites.

redispersed by gentle shaking. Therefore these magnetic properties are critical in the applications of the biomedical and bioengineering fields.

Influence of The Fe$_3$O$_4$ Content on The Saturated Magnetization

The magnetization curves for magnetic Fe$_3$O$_4$/P(MAH-co-AA) nanocomposite with different Fe$_3$O$_4$ dosages are shown in Fig. 9. It can be seen from the magnetization curves that the saturation magnetization (Ms) of the MNPs increased from 11.8 to 57.4 emu g^{-1}, when Fe$_3$O$_4$ content increased from 1 to 7 wt% of polymer shell. It indicated that more Fe$_3$O$_4$ nanoparticles being trapped in the polymer matrix. These data also indicated that the Fe$_3$O$_4$ content in composites systems can be varied. In addition, the increase in Ms can be attributed to the increase in particle size which reduced the surface area. It is clear that

the energy of a magnetic particle in an external field is proportional to its size via the number of magnetic molecules in a single magnetic domain. When this energy becomes comparable to the thermal energy, thermal fluctuations will significantly enhance the total magnetic moment at a given field [17]. The saturation magnetization value of 16.3 emu g^{-1} was sufficient for magnetic separation with a conventional magnet [18]. Therefore, the magnetization value achieved with the 5 wt% Fe$_3$O$_4$ content of the polymer particles was high enough for magnetic separation.

Optimization of Polymer Shell onto the Surface of Magnetic Nanoparticles

The magnetization curves of the polymer-coated Fe$_3$O$_4$ nanocomposites at different concentration of polymer recorded with VSM
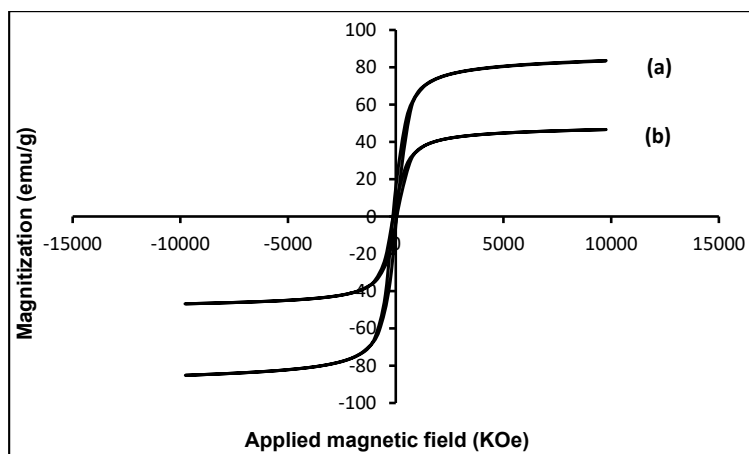

Fig. 8 Magnetization curve of (a) Fe$_3$O$_4$-MNPs, and (b) magnetic Fe$_3$O$_4$/P(MAH-co-AA) core/shell nanocomposites.
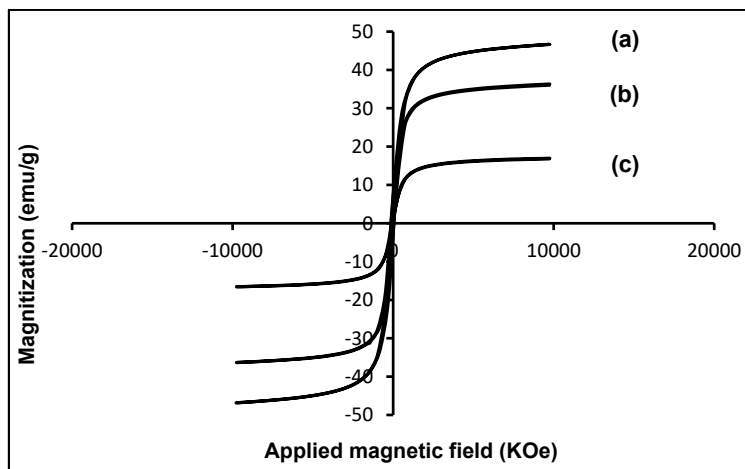

Fig. 9. Magnetization curve for magnetic Fe$_3$O4/P(MAH-co-AA) nanocomposite synthesized at various Fe$_3$O$_4$ concentration: (a) 7%, (b) 5%, (c) 3%, and (d) 1 wt%.
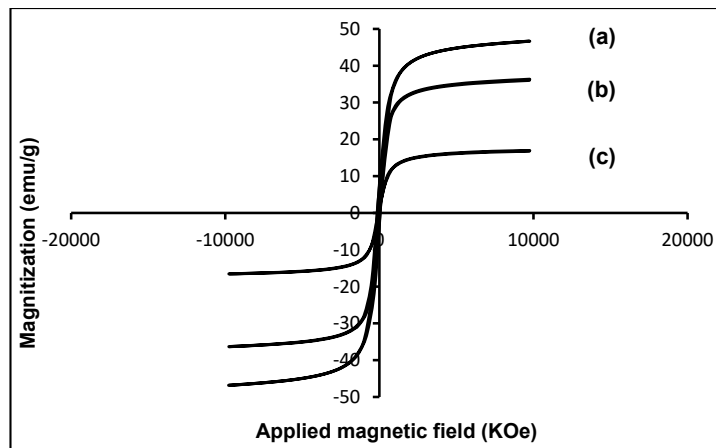
Fig. 10 Magnetization curve for magnetic Fe_3O_4/P(MAH-co-AA) nanocomposite synthesized at various polymer concentration: (a) 1:4, (b) 1:5, and (c) 1:6 wt%.

at room temperature are shown in Fig. 10. It can be seen that the saturation magnetization of nanocomposites significantly decreases from 46.2 to 14.2 emu g^{-1} with the increase in polymer concentration. Because the weights of nanoparticles used for the measurement of magnetic properties were constant and the decrease of saturation magnetization was due to the increased amount of polymer incorporated in the polymer-coated magnetite, thus the increase in the mass of polymer results in the decrease in the magnetic strength of the nanocomposite.

The reduction of the saturation magnetization can be explained by the presence of polymer on the surface of Fe_3O_4 nanoparticles which may generate a magnetically dead layer so any crystalline disorder within the surface layer cause to a significant decrease in the saturation magnetization of nanoparticles [19]. The saturation magnetization of Fe_3O_4/P(MAH-co-AA) (1:4), Fe_3O_4/P(MAH-co-AA) (1:5) and Fe_3O_4/P(MAH-co-AA) (1:6) were 46.2, 31.6 and 14.2 emu g^{-1}, respectively.

According to previous part the saturation magnetization value achieved with the Fe_3O_4/P(MAH-co-AA) magnetic nanocomposite below 6 wt% was high enough for magnetic separation. On the other hand, the use of polymer above 5 wt% of Fe_3O_4 duo to decrease in Ms is not sufficient for magnetic separation.

The result demonstrates that the magnetic properties of the magnetic Fe_3O_4/P(MAH-co-AA) nanoparticles are strongly influenced by the polymer shell thickness. In addition, the magnetic properties of the nanocomposite can be easily controlled by varying the starting polymerization during fabrication [20].

CONCLUSION

In this study a magnetic nanocomposite has been successfully synthesized by dispertion polymerization method with core/shell structure. The coated OA molecules as surfactant on the nanoparticles surface leads to highly dispersed and high entrapment efficiency of magnetic into a polymer and also smaller particle size. The TEM images reveal that the Fe_3O_4 and Fe_3O_4/P(MAH-co-AA) core/shell nanoparticles are roughly cubic in shape and uniform in size with a mean diameter of 9.41 nm for Fe_3O_4 nanoparticles and after surface polymerization the mean diameter of nanoparticles (core/shell) increased to 17.09 nm. The X-ray diffraction pattern revealed that the structure and crystallity of Fe_3O_4 core was not changed significantly after coating.

The magnetic behaviors of polymer-coated magnetite nanoparticles exhibit superparamagnetism. All examinations have demonstrated that the Fe_3O_4 nanoparticles coated with surfactants oleic acid act as a core and the polymer layer of P(MAH-co-AA) formed on the Fe_3O_4 surface as a shell.

ACKNOWLEDGEMENTS

CONFLICT OF INTEREST

The authors declare that there are no conflicts

of interest regarding the publication of this manuscript.

REFERENCES

1. Faraji M, Yamini Y, Rezaee M. Magnetic Nanoparticles: Synthesis, Stabilization, Functionalization, Characterization, and Applications. J. Iran. Chem. Soc., 2010; 7: 1-37.

2. Shan G, Surampalli R, Tyagi R, Zhang T. Nanomaterials for Environmental Burden Reduction, Waste Treatment, and Nonpoint Source Pollution Control: A Review. Front. Environ. Sci. Engin. China, 2009; 3: 249–264.

3. Wu Y, Zhang T, Zheng Z, Ding X. Peng Y. A Facile Approach to Fe_3O_4@Au Nanoparticles with Magnetic Recyclable Catalytic Properties. Mater. Res. Bull., 2010; 45: 513-517.

4. Vaia R.A, Giannelis E.P. Liquid Crystal Polymer Nanocomposites: Direct Intercalation of Thermotropic Liquid Crystalline Polymers in to Layered Silicates. Polymer, 2001; 42: 1281-1285.

5. Wei W, Zhaohui W, Taekyung Y, Changzhong J, Woo-Sik K. Recent Progress on Magnetic Iron Oxide Nanoparticles: Synthesis, Surface Functional Strategies and Biomedical Applications. Sci. Technol. Adv. Mater., 2015; 16: 43-49.

6. Orive G, Hernandez R.M, Gascon A.R, Domınguez-Gil A, Pedraz J.L. Drug Delivery in Biotechnology: Present and Future. Curr. Opin. Biotechnol., 2003; 14: 659–664.

7. Sun Z.H, Wang L.F, Liu P.P, Wang S.C, Sun B, Jiang D.Z, Xiao F.S. Magnetically Motive Porous Sphere Composite and Its Excellent Properties for the Removal of Pollutants in Water by Adsorption and Desorption Cycles. Adv. Mater., 2006; 18:1968-1971.

8. Azizi S, Mahdavi Shahri M, Mohamad R. Green Synthesis of Zinc Oxide Nanoparticles for Enhanced Adsorption of Lead Ions from Aqueous Solutions: Equilibrium, Kinetic and Thermodynamic Studies. Molecules, 2017; 22: 831.

9. Mahdavi M, Ahmad M.B, Haron M.J, Namvar F, Nadi B, Ab Rahman M.Z, Amin J. Synthesis, Surface Modification and Characterisation of Biocompatible Magnetic Iron Oxide Nanoparticles For Biomedical Applications. Molecules, 2013; 18: 7533-7548.

10. Kazemi N. Mahdavi Shahri M. Magnetically Separable and Reusable $CuFe_2O_4$ Spinel Nanocatalyst for the O-Arylation of Phenol with Aryl Halide under Ligand-Free Condition. J. Inorg. Organomet. Polym., 2017; 27: 1-10.

11. Mahdavi M, Ahmad M.B, Haron M.J, Gharayebi Y, Shameli K, Nadi B. Fabrication and Characterization of SiO_2/(3-Aminopropyl) Triethoxysilane-Coated Magnetite Nanoparticles for Lead (II) Removal from Aqueous Solution. J. Inorg. Organ. Polym. Mater., 2013; 23: 599-607.

12. Halyna O, Larysa D, Viktor T. Synthesis and Application of Macrophotoinitiators Obtained Via Benzoin Tethering with Copolymers of Maleic Anhydride. Chem. Chem. Technol., 2013; 7: 125-130.

13. Yew Y.P, Shameli K, Miyake M, Kuwano N, Ahmad Khairudin N.B, Mohamad S.E, Lee X.K. Green Synthesis of Magnetite (Fe_3O_4) Nanoparticles Using Seaweed (Kappaphycus alvarezii) Extract. Nano. Res. Lett., 2016; 11: 276.

14. Yan F, Li J, Zhang J. Preparation of Fe_3O_4/Polystyrene Composite Particles from Monolayer Oleic Acid Modified Fe3O4 Nanoparticles Via Miniemulsion Polymerization. J. Nanop. Res., 2009; 11: 289–296.

15. Guo L, Liu G, Hong R.Y, Li H.Z. Preparation and Characterization of Chitosan Poly(acrylic acid) Magnetic Microspheres. Mar. Drugs, 2010; 8: 2212-2222.

16. Qu J, Liu G, Wang Y, Hong R. Preparation of Fe_3O_4–Chitosan Nanoparticles Used for Hyperthermia. Adv. Powder Technol., 2010; 21: 461–467.

17. Liao M.H, Chen D.H. Preparation and Characterization of a Novel Magnetic Nano-Adsorbent J. Mater. Chem., 2002; 12: 3654-3659.

18. Ma Z, Guan Y, Liu H. Synthesis and Characterization of Micron-Sized Monodisperse Superparamagnetic Polymer Particles with Amino Groups. J. Polym. Sci. Part A: Polym. Chem., 2005; 43: 3433–3439.

19. Li G, Jiang Y, Huang K, Ding P, Chen J. Preparation and Properties of Magnetic Fe_3O_4–Chitosan Nanoparticles. J. Alloy. Compd., 2008; 466: 451-456.

20. Zhao X, Wang J, Wu F, Wang T, Cai Y, Shi Y, Jiang G. Removal of Fluoride from Aqueous Media by Fe_3O_4@Al(OH)$_3$ magnetic nanoparticles. J. Hazard. Mater., 2010; 173: 102–109.